Opt Quant Electron (2017)49:170
DOI 10.1007/s11082-017-1002-y

Nonsequential double ionization of Xe by mid-infrared laser pulses

Xiaomeng Ma[1] · Min Li[1] · Yueming Zhou[1] · Peixiang Lu[1,2]

Received: 11 February 2017 / Accepted: 23 March 2017

Abstract With the three-dimensional semiclassical ensemble model, we studied the correlated electron dynamics in strong-field nonsequential double ionization of Xe by mid-infrared laser pulses over a wide range of laser intensities. Numerical results show that the correlated electron momentum distribution exhibits the strong back-to-back pattern at the lower laser intensity. It evolves into the side-by-side behavior as the laser intensity increases and presents the experimentally observed crosslike shape at high laser intensity. Different from the case of near-infrared region where recollision mainly occurs at the first returning, at the mid-infrared region recollision dominantly occurs at the later returnings. The windows of initial transverse velocity for the various multiple-returning recollision trajectories are different and are unambiguously determined by this semiclassical ensemble model.

Keywords Nonsequential double ionization · Electron correlations · Mid-infrared laser pulses

1 Introduction

Nonsequential double ionization (NSDI) has been a hot topic in strong-field atomic and molecular physics since the first observation of the enhanced double ionization yield (I'Huillier et al. 1983). During the past two decades, a large number of experimental and

✉ Yueming Zhou
zhouymhust@hust.edu.cn

Xiaomeng Ma
maxiaomeng@hust.edu.cn

Min Li
mli@hust.edu.cn

[1] School of Physics, Huazhong University of Science and Technology, Wuhan 430074, People's Republic of China

[2] Laboratory of Optical Information Technology, Wuhan Institute of Technology, Wuhan 430205, People's Republic of China

Published online: 31 March 2017

theoretical studies have been performed on NSDI (Fittinghoff et al. 1992; Walker et al. 1994; Moshammer et al. 2000; Rudenko et al. 2004; Liu et al. 2004; Weber et al. 2000; Weckenbrock et al. 2003; Lein et al. 2000; Becker and Faisal 2000; Hao et al. 2014; Maxwell et al. 2016; Fu et al. 2001; Bauer 1997; Panfili et al. 2001; Ma et al. 2016; Huang et al. 2017; Wang et al. 2017a) and it is well known that the recollision process is the responsible mechanism (Corkum 1993). In the recollision process, the first electron is released by the laser field through tunneling, and then is accelerated by the oscillating field and impelled back to the core when the electric field changes its sign, leading to the second electron ionized directly (RDI) or excited with subsequent field ionization (RESI) (Feuerstein et al. 2001). Because of the recollision, the electron pairs display a distinctive correlation and the details of the correlated electron dynamics have been revealed from the correlated electron momentum distribution (CEMD) (Weber et al. 2000; Weckenbrock et al. 2003). For example, it has been shown that the electron correlations in NSDI strongly depend on laser intensity. At intensities well below the recollision threshold, the CEMD shown a back-to-back behavior (Liu et al. 2008), which was attributed to the time delay between the emissions of the correlated electrons (Haan et al. 2008b). At moderate intensity, the CEMD presented a pronounced V-like (or called as fingerlike) shape (Staudte et al. 2007). Theoretical studies have demonstrated that both the nuclear attraction and final-state electron repulsion are responsible for this structure (Haan et al. 2008a; Ye et al. 2008; Chen et al. 2010). At a much higher laser intensity, the V-like structure was also observed in NSDI of He (Rudenko et al. 2007). However, neither the nuclear attraction nor the final-state electron repulsion accounts for this structure. It is the asymmetric energy sharing during recollision that results in the V-like structure at high laser intensities (Zhou et al. 2010). Recently, this structure was also observed for NSDI of Ar and N_2 by the few-cycle pulses at high laser intensity region (Bergues et al. 2012; Kübel et al. 2013), which is also ascribed to the asymmetric energy sharing (Kübel et al. 2013; Huang et al. 2016a).

Most of previous works on NSDI are done in the near-infrared (NIR) region, the fundamental wavelength of Ti:Sapphire laser systems. The development of ultrafast laser technology has pushed the wavelength into the mid-infrared (MIR) region (Agostini and DiMauro 2008; Liu et al. 2016; Tanaka et al. 2016). For the case of longer wavelengths, the microscopic dynamic of correlated electron in NSDI is different from the case of NIR region (Herrwerth et al. 2008; Alnaser et al. 2008; DiChiara et al. 2012; Huang et al. 2016b; Li et al. 2016). It was observed that at longer wavelengths, the dip of the characteristic double-hump structure in the longitudinal momentum spectrum of Ne^{2+} and N_2^{2+} becomes more pronounced (Herrwerth et al. 2008; Alnaser et al. 2008). Especially for Ar, in which the double-peak structure is very faint at 800 nm field (Liu et al. 2008; Rudenko et al. 2008), it becomes as clear as that in Ne at 1300 nm (Herrwerth et al. 2008; Alnaser et al. 2008). These results indicate the contribution of RDI pathway at longer wavelengths is strongly enhanced, as compared to the case at 800 nm (DiChiara et al. 2012; Tang et al. 2012). More remarkably, for NSDI of Xe by MIR pulses at 3100 nm, the CEMDs of electrons is mainly distributed in the first and third quadrants and displays a crosslike shape (Wolter et al. 2015; Pullen et al. 2016). This is totally different from the case by the 800 nm fields where the electrons are almost uniformly located in the four quadrants and show nonstructural distribution (Sun et al. 2014). Theoretical studies based on a semiclassical model have discussed that this nonstructural distribution at 800 nm field might be due to the electron shielding effect in the high-Z atoms (Yuan et al. 2016). However, the details of microscopic dynamics of NSDI driven by these long wavelength laser pulses remain unclear.

In this paper we perform a systematic investigation on NSDI of Xe by the 3000 nm pulses over a wide range of laser intensities. With a three-dimensional (3D) semiclassical ensemble model (Fu et al. 2001), the experimentally observed crosslike structure in the CEMD is well reproduced. Back analysis of the classical trajectories shows that the two electrons prefer asymmetric energy sharing at recollision in the MIR region, which is responsible for the observed crosslike shape. Our calculations predict that the crosslike shape disappears when the laser intensity decreases and finally the CEMD evolves into a back-to-back emission behavior at low laser intensity. More surprisingly, back tracing of the classical trajectory shows that in the MIR region recollision mainly occurs at later returnings. This is different from the case in the NIR region where recollision dominantly occurs at the first returning. In the multiple-returning recollision process, the Coulomb focusing effect plays an important role. In addition, the initial transverse velocity windows of the first tunneling electrons are found with this semicalssical ensemble model.

2 The semiclassical ensemble model

Accurate description of the two-electron system in the strong laser field requires numerically solving the time-dependent Schrödinger equation. However, the computational demand of this method is huge (Parker et al. 2006; Hu 2013), especially for the wavelengths at MIR region. In the past decades, a multitude of theoretical approaches have been developed (see de Morisson Faria and Liu 2011 and the references therein). Among the existing methods, classical (semiclassical) method (Fu et al. 2001; Haan et al. 2006; Mauger et al. 2009; Zhou et al. 2012; Tong et al. 2017; Xu et al. 2015) has been proved to be one of the most effect approaches in studying NSDI, though some quantum effects, such as the interference in NSDI (Maxwell et al. 2016) cannot been captured. It has been shown that the classical methods are very successful not only in interpreting the experimental results (Ye et al. 2008; Zhou et al. 2010, 2011a; Wang and Eberly 2009) but also in predicting new phenomena (Zhou et al. 2011b; Tong et al. 2015). For instance, with a classical model we have predicted the back-to-back electron emission in NSDI by orthogonal two-color fields which has been confirmed by the recent experiment (Zhang et al. 2014). The subcycle electron emission in sequential double ionized predicted by a classical model has been successfully observed in experiment (Schöffler et al. 2016). More importantly, classical methods have the advantage of back-tracing the classical trajectories, through which the underlying process can be intuitively presented (Ho et al. 2005). Thus, in this paper we employ the 3D semiclassical ensemble model (Fu et al. 2001) to study the electron dynamics of NSDI in the MIR laser fields.

In this semiclassical ensemble model, the first electron is ionized through tunneling with a probability according to tunneling theory (Ammosov et al. 1986). The tunneling electron has zero parallel velocity and a Gaussian transverse (with respect to the direction of electric field) velocity distribution (Delone and Krainov 1991). For the second electron, the initial position and momentum are depicted by microcanonical distribution. The subsequent evolution of the two electrons in the combined Coulomb potential and the laser fields is described by the classical Newtonian equation (atomic units are used throughout until stated otherwise):

$$\frac{d^2\mathbf{r}_i}{dt^2} = -\boldsymbol{\varepsilon}(t) - \nabla[V_{ne}(\mathbf{r}_i) + V_{ee}(\mathbf{r}_1, \mathbf{r}_2)], \tag{1}$$

where the index i denotes the label of the two electrons, and $\mathbf{r}_i$ refers to the electronic coordinates. $\boldsymbol{\varepsilon}(t) = \varepsilon_0 f(t)\cos(\omega t)\hat{\mathbf{x}}$ is the laser field, with ε_0, ω the amplitude, frequency of the laser electric field, respectively. $f(t)$ is the pulse envelope which has a constant amplitude for the first eight cycles and is turned off with a two-cycle ramp. $V_{ne}(\mathbf{r}_i) = -2/\sqrt{\mathbf{r}_i^2 + a^2}$ and $V_{ee}(\mathbf{r}_1, \mathbf{r}_2) = 1/\sqrt{(\mathbf{r}_1 - \mathbf{r}_2)^2 + b^2}$ are the interaction potential between the nucleus and electrons, and between two electrons, respectively. The soft parameter a is set to 2.0 to avoid autoionization and b is set to 0.01 (Haan et al. 2008b; Zhou et al. 2010).

The weight of each trajectory is evaluated by $w(t_0, v_{\perp 0}^i) = w(t_0)w(v_{\perp 0}^i)$ (Fu et al. 2001), in which

$$w(t_0) = \left(\frac{2(-2I_{p1})^{1/2}}{|\boldsymbol{\varepsilon}|}\right)^{\frac{2}{\sqrt{-2I_{p1}}}-1} \exp\left(\frac{-2(-2\mathrm{I_{p1}})^{3/2}}{3|\boldsymbol{\varepsilon}|}\right), \tag{2}$$

$$w(v_{\perp 0}^i) = \frac{v_{\perp 0}^i}{|\boldsymbol{\varepsilon}|}\exp\left(-\frac{(v_{\perp 0}^{\mathrm{i}})^2(-2\mathrm{I_{p1}})^{1/2}}{|\boldsymbol{\varepsilon}|}\right). \tag{3}$$

$w(t_0)$ is the instantaneous tunneling probability and $w(v_{\perp 0}^i)$ is the distribution of initial transverse velocity $v_{\perp 0}^i$. In our calculations, the first and second ionization potentials are chosen as $I_{p1} = -0.45$ a.u. and $I_{p2} = -0.78$ a.u., respectively, to match those of Xe. The laser frequency is $\omega = 0.015$ a.u., corresponding to the wavelength of 3000 nm. Several million weighted classical two-electron trajectories are traced from the tunneling moment to the end of the pulse, resulting in more than 10^4 DI events for statistics.

3 Results and discussions

Figure 1 presents the CEMDs along the polarization direction for NSDI of Xe, where the laser intensities are (a) 0.06×10^{14}W/cm^2, (b) 0.1×10^{14} W/cm^2, (c) 0.4×10^{14} W/cm^2, and (d) 1.0×10^{14}W/cm^2, respectively. At the low intensity, as shown in Fig. 1a, the spectrum exhibits an anticorrelated behavior, i.e., the electron pairs prefer to emit into the opposite hemispheres. When the laser intensity increases, the electrons are mainly distributed in the first and third quadrants, displaying a prominent correlated behavior, as shown in Fig. 1b. At the higher intensity, as shown in Fig. 1c, the distribution is also mainly located in the first and third quadrants and shows a clear crosslike shape. This crosslike shape has been observed in recent experiments (Wolter et al. 2015; Pullen et al. 2016), confirming the validity and accuracy of this semiclassical model. As the intensity further increases, the crosslike shape becomes more obvious, as shown in Fig. 1d. It is worth noting that at the NIR region, this transition from anticorrelated to correlated behavior has been observed for Ar (Liu et al. 2008). However, for Xe, this transition has not been observed and it was found that the CEMD shows a universal nonstructural distribution over a wide range of laser intensities (Sun et al. 2014).

To explore the responsible electron dynamics, we take advantage of the semiclassical model by back-tracing the NSDI trajectories, which enables us easily to determine the recollision time and double ionization time. Here, the recollision time is defined as the instant of closest approach of the two electrons after the tunneling of the first electron, and the double ionization time is defined as the instant when both electrons achieve positive energies (Haan et al. 2008b; Zhou et al. 2011b). Back tracing of the classical trajectories

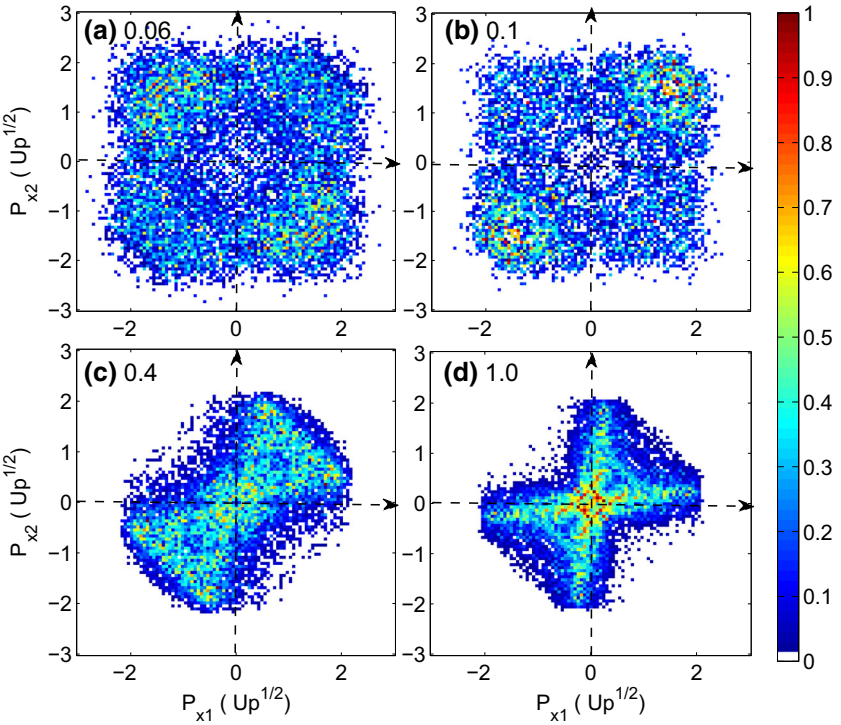

Fig. 1 The CEMD in the parallel direction (parallel to the laser polarized direction) for NSDI of Xe by the 3000 nm laser pulses. The laser intensities are **a** 0.06×10^{14} W/cm^2, **b** 0.1×10^{14} W/cm^2, **c** 0.4×10^{14} W/cm^2 and **d** 1.0×10^{14} W/cm^2. (Color figure online)

shows that usually double ionization does not occur immediately after recollision. For most of the NSDI events there is some time delay between double ionization and recollision. Figure 2 shows this time delay. According to the simple-man model, the maximum recollision energy in NSDI is about $3.17U_p$ (U_p is the ponderomotive energy) (Corkum 1993). At the low laser intensity of 0.06×10^{14} W/cm^2, the maximum recollision energy of $3.17U_p$ is about 0.59 a.u., which is much smaller than the ionization potential of the second electron. Thus, NSDI can only occur through the RESI pathway. As shown in Fig. 2a, the time delay between the double ionization and recollision is about 0.25 optical cycle (o.c.), indicating the main process indeed is RESI (Feuerstein et al. 2001). In this process, the first electron is usually ionized before the first peak of the electric field after recollision and the second electron is released after the first peak of electric field. In this case, the two electrons achieve final longitudinal momenta with different directions, resulting in the anticorrelated behavior in the CEMD (Haan et al. 2008b; Zhou et al. 2011a).

At the intensity of 0.1×10^{14} W/cm^2, the maximum returning energy $3.17U_p \approx 0.98$ a.u. is higher than the second ionization potential of Xe. Figure 2b shows that still there is time delay between double ionization and recollision, meaning that RESI dominates the NSDI events. Even for higher intensities, a significant part of the NSDI events occur through the RESI, as shown in Fig. 2c, d. For most of the events, the time delay is within 0.25 o.c., indicating that both electrons are ionized before the first peak of electric field

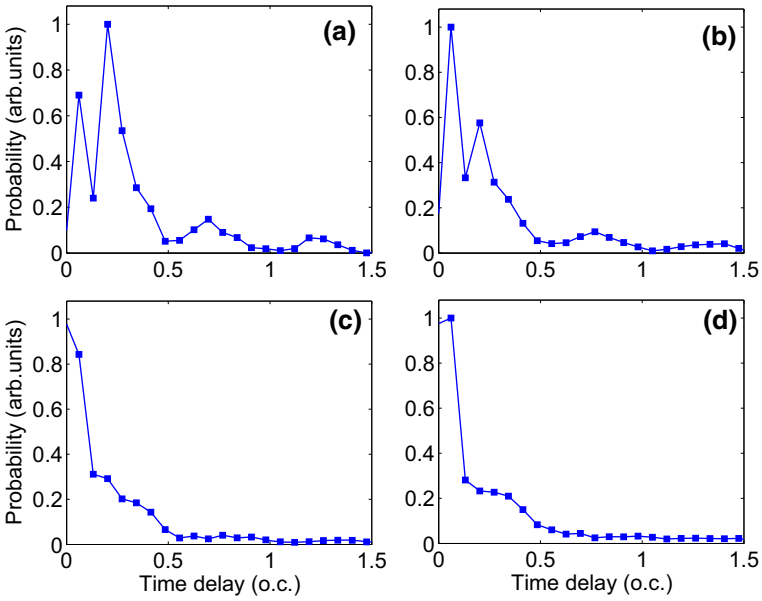

Fig. 2 Time delay between double ionization and recollision. **a–d** correspond to the events in Fig. 1a–d, respectively. (Color figure online)

after recollision. In this case, the two electrons emit into the same hemisphere and the CEMD exhibits the correlated behavior (Zhou et al. 2011b), as shown in Fig. 1b–d.

The crosslike (or V-like) structure in Fig. 1c, d has been experimentally observed in NSDI of He, Ar and N_2 by NIR laser pulses with very high laser intensities. Theoretical studies have revealed that asymmetric energy sharing at recollision is responsible for this structure (Zhou et al. 2010). To identify the mechanism for the crosslike structure in NSDI of Xe by the MIR laser pulses, in Fig. 3 we plot the energy distributions of the two electrons at time 0.02 o.c. after recollision. Here, the energy of each electron is defined to contain the kinetic energy, potential energy of the electron-ion interaction, and half of electron-electron potential energy (Haan et al. 2008b; Zhou et al. 2011a). Figure 3 shows that for all of intensities the distributions are away from the main diagonal, indicating the asymmetric energy sharing during recollision. Especially for the high laser intensities (Fig. 3c, d), the first electron only excites the second electron though its returning energy is much higher than the ionization potential of the second electron. While the first electron itself possesses most of the returning energy. This process can explain the remarkable crosslike structure in Fig. 1c, d. We note that the asymmetric energy sharing in the MIR region is much more extreme than the case in the NIR region. The reason might be due to the spreading of the electron wave packet. For the laser pulses with longer wavelength, the electron wave packet spreads more widely and thus the impact parameter is larger. Consequently, the soft recollision where the returning electron only transfers a small part of its energy to the bounded electron, is more prevalent.

A more interesting issue is manifested in the transverse momentum distribution. In the semiclassical ensemble model, the two electrons are distinguishable. In Fig. 4 we separately plotted the final transverse momentum spectra of the first and second electrons. At the relatively low laser intensities, as shown in Fig. 4a, b, the spectra of the two electrons

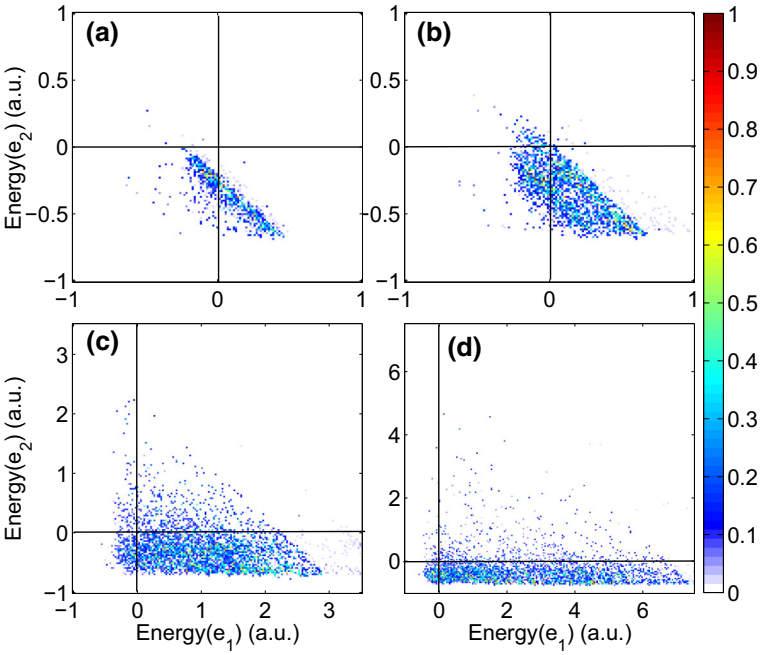

Fig. 3 Distributions of the energy of the bound electron versus the recolliding electron at time 0.02 o.c. after recollision. **a–d** correspond to the events in Fig. 1a–d, respectively. (Color figure online)

are almost the same. While for the higher laser intensities, shown in Fig. 4c, d, the spectra of the first electron are much broader than those of the second electron. These behaviors can be understood as following. At the relatively low laser intensities (Fig. 4a, b), both electrons are ionized through excited states or leave the ion with near-zero initial momentum after recollision. Due to the small initial transverse momentum and Coulomb focusing effect, the final transverse momentum distributions are narrow and exhibit a cusp-like structure (Zhou et al. 2009; Ivanov et al. 2016). For higher laser intensities (Fig. 4c, d), because of the dramatic asymmetric energy sharing during recollision, the second electron can only be excited or ionized with a very small initial momentum. Thus the final transverse momentum distributions are narrow, similar to the case of the lower laser intensities. However, the first electron possesses a larger energy after recollision, and it can obtain a considerable transverse momentum during recollision. Because of the larger initial momentum after recollision, the first electron passes through the core more quickly and thus the Coulomb focusing effect is negligible. Therefore, the final transverse momentum distribution of the first electron is wider. Because the transverse momentum is not covered by the large momentum taken from the laser field, it keeps more subtleties of the recollision dynamics in NSDI. Therefore this difference in the transverse momentum distributions of the two electrons is a convincing evidence of asymmetric energy sharing and we hope it could be confirmed in future experiments.

To reveal more details of the recollision dynamics of NSDI, in Fig. 5 we present the distributions of the traveling time of the tunneled electron, which is defined as the time delay between recollision and tunneling ionization of the first electron. Here the recollision time was obtained by back tracing the trajectories. According to the recollision picture, the

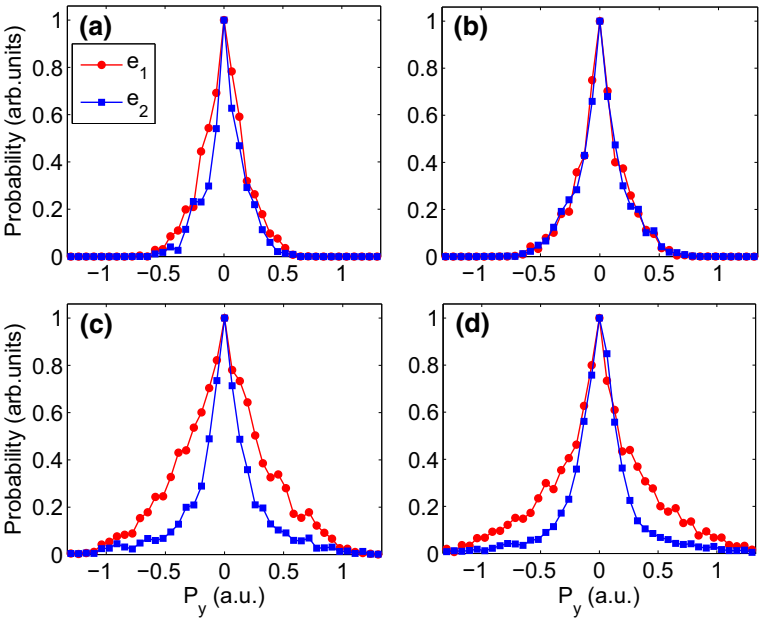

Fig. 4 **a–d** The final transverse momentum distributions of the first (*red circle*) and second (*blue square*) electrons for the events from Fig. 1a–d, respectively. Here the first and second electrons refer to the returning and bounded electrons, respectively. (Color figure online)

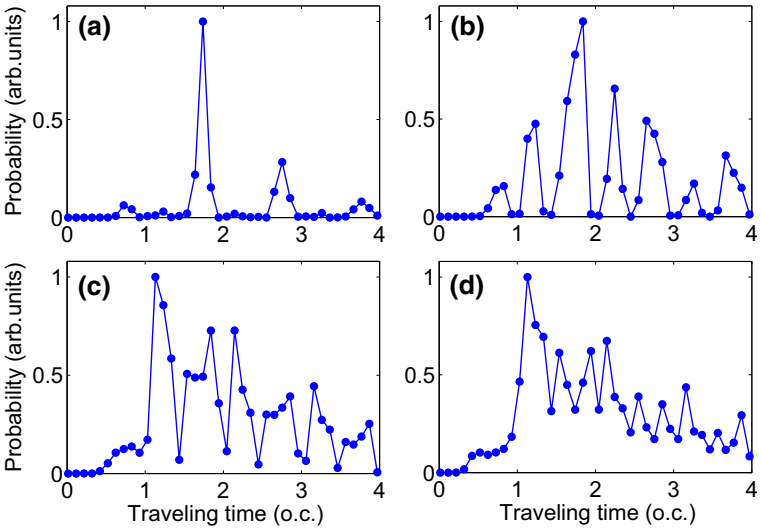

Fig. 5 **a–d** Traveling time distributions for the NSDI trajectories in Fig. 1a–d, respectively. The traveling time is defined as the time delay between recollision and the tunneling ionization of the first electron. (Color figure online)

traveling time is about 0.7 o.c. if recollision occurs at the first returning (Corkum 1993). In the NIR region, it is the first-returning recollision that dominates the recollision phenomena (Zhou et al. 2016; He et al. 2016; Zhai et al. 2016, 2017; Zhu et al. 2016; Qin and Zhu

2017; Li et al. 2017; Zhang et al. 2017; Wang et al. 2017a; Liu et al. 2017). However, in the MIR region, as shown in Fig. 5, the distributions exhibit several peaks located at 0.7 o.c., 1.2 o.c., 1.7 o.c. et al., which correspond to the recollision occurring at the first, second and third returnings, respectively. The later peaks are much stronger than the first peak, meaning that the multiple-returning recollision dominates over the recollision occurring at the first returning in the MIR region. The proportion of the multiple-returning recollision trajectories is larger than 95 percents. This is totally different from NSDI at NIR region where the recollision mainly occurs at the first returning (Ye et al. 2008; Haan et al. 2006; Zhou et al. 2011a). It is worth to mention that the multiple-returning recollision has been observed in the previous experiment on above threshold ionization (Hickstein et al. 2012). However, it was shown that multiple-recollision only appears at the low-energy part of the photoelectron spectrum, which corresponds to the near-zero energy recollision. In NSDI, the recollision energy is much higher. Our results indicate that multiple-returning recollision has a dominant contribution in this two-electron process, which has not been observed in the above threshold ionization experiment.

Figure 5 shows that the traveling time distribution changes with laser intensity. At the lowest laser intensity (shown in Fig. 5a), the peak corresponding to the third returning dominates, while at the higher laser intensities, the peak of the second returning is stronger. This is due to the fact that at low laser intensities the recollision energy is the main factor effecting NSDI. The maximum recollision energy of the second returning is about $1.54U_p$ (Lewenstein et al. 1994), which is not high enough to induce the ionization of the second electron at the lowest laser intensity. The third returning, which possesses higher recollision energy, has the main contribution to double ionization. At the higher laser intensities, the recollision energy at the second returning is high enough to ionize the second electron, and thus the second-returning recollision is more prevalent.

The semiclassical model enables us to determine the initial transverse velocity of the first electron at tunneling. We first classified the NSDI events according to the number of the returning at which recollision occurs. In Fig. 6 we separately present the initial transverse velocity ($v^i_{\perp 0}$) distributions for the NSDI events where recollision occurs at the first, second, third and forth returnings. It is shown that the corresponding initial transverse velocity increases with the number of returnings. To understand this issue we display an illustrative trajectory in Fig. 7. Figure 7a–c show, respectively, the time evolution of the $\hat{\mathbf{x}}$-component of coordinates, the $\hat{\mathbf{y}}$-component of coordinates, and the transverse velocities v_y. The red and gray lines denote the first and the second electrons, respectively. Because of the initial transverse velocity, the tunneled electron misses the core during the first and the second returnings (see Fig. 7b). However, every time when it passes by the core, the Coulomb attraction exerts a transverse momentum toward the core to the electron (Fig. 7c), which makes the electron move gradually to the core and the effective recollision finally happens at the third returning. For a larger initial transverse velocity, the electron can be focused to the core and result in an effective recollision only after it passes by the core several more times. This is the reason why the corresponding initial transverse velocity increases with the number of returnings. This implicitly indicates the important role of Coulomb focusing in the transverse motion of the returning electron in the MIR region.

Another interesting feature in Fig. 6 is that the corresponding velocity decreases as the laser intensity increases. For example, for the third-returning recollision events, the initial transverse velocity is about 0.08 a.u. at the intensity of 0.06×10^{14} W/cm^2 and it decreases to 0.04 a.u. at the intensity of 0.4×10^{14} W/cm^2. This can also be interpreted as the effect

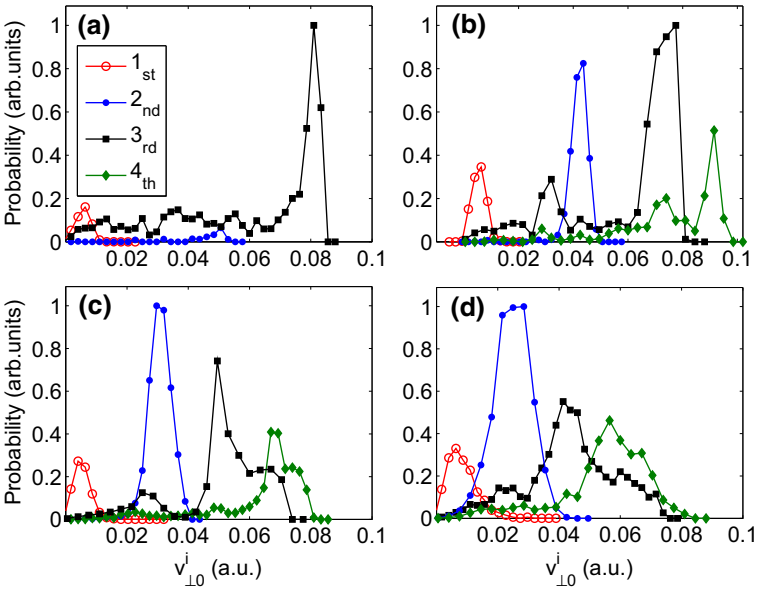

Fig. 6 The initial transverse velocity $v^i_{\perp 0}$ distributions at tunneling ionization. Here we separately plotted the NSDI events where recollision occurs at the first, second, third and forth returning, respectively (as indicated by the legend in **a**). **a**–**d** correspond to the events in Fig. 1a–d, respectively. (Color figure online)

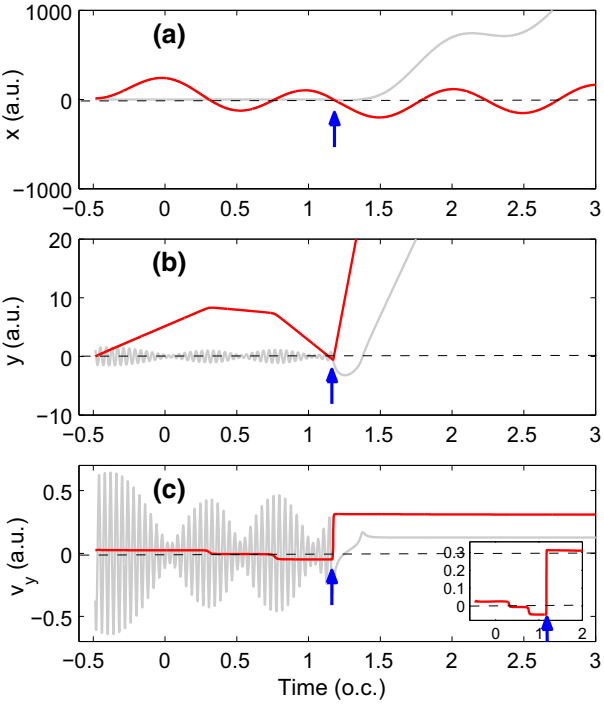

Fig. 7 An illustrated classical trajectory. The *red* and the *gray* curves represent the first and the second electrons, respectively. **a** and **b** display the time evolution of the coordinate $\hat{\mathbf{x}}$ and $\hat{\mathbf{y}}$ of each electron. **c** shows the time evolution of the velocity v_y. The laser pulse is polarized along the $\hat{x}$-axis. The inset in (**c**) enlarges the left part of the main panel. In the trajectory the effective recollision occurs at the third returning, as indicated by the *blue arrows*. (Color figure online)

of Coulomb focusing. For the higher laser intensity, the electron returns back with a larger momentum and passes by the core more quickly. Consequently, the action time of coulomb interaction is shorter and thus the focusing effect is smaller compared to the case of lower laser intensity. In other words, for the trajectories with the same number of returnings, the Coulomb focusing effect can only compensate a smaller initial transverse velocity, as compared to the lower laser intensity.

4 Conclusion

In summary, we have investigated NSDI of Xe by the MIR laser pulses with the semiclassical ensemble model. Our calculations well reproduced the experimentally observed crosslike shape in the CEMD and predicted its dependence on the laser intensity. The responsible mechanisms are explored by back tracing the classical trajectories. Most interestingly, our results show that recollision of NSDI is more likely to occur at the later returnings than the first returning in the MIR region. This is very different from NSDI by NIR laser pulses where recollision dominantly occurs at the first returning. A proper nonzero initial transverse velocity of the tunneled electron is necessary for these multiple-returning recollision induced NSDI events. The windows of the initial transverse velocity for the various multiple-return recollision trajectories are determined by this semiclassical ensemble model. In addition, we demonstrated that in these multiple-returning recollision processes, the Coulomb focusing effect plays an important role.

Acknowledgements This work was supported by the National Natural Science Foundation of China under Grant Nos. 11622431, 61405064 and 11234004. Numerical simulations presented in this paper were carried out using the High Performance Computing Center experimental testbed in SCTS/CGCL (see http://grid.hust.edu.cn/hpcc).

References

Agostini, P., DiMauro, L.F.: Atoms in high intensity mid-infrared pulses. Contemp. Phys. **49**, 179–197 (2008)

Alnaser, A.S., Comtois, D., Hasan, A.T., Villeneuve, D.M., Kieffer, J., Litvinyuk, V.: Strong-field nonsequential double ionization: wavelength dependence of ion momentum distributions for neon and argon. J. Phys. B **41**, 031001 (2008)

Ammosov, M.V., Delon, N.B., Krainov, V.P.: Tunnel ionization of complex atoms and atomic ions in electromagnetic field. Zh. Eksp. Teor. Fiz. **91**: 2008–2013 (1986). [Sov. Phys. JETP **64**, 1191-1194 (1986)]

Bauer, D.: Two-dimensional, two-electron model atom in a laser pulse: exact treatment, single-active-electron analysis, time-dependent density-functional theory, classical calculations, and nonsequential ionization. Phys. Rev. A **56**, 3028–3039 (1997)

Becker, A., Faisal, F.H.M.: Interpretation of momentum distribution of recoil ions from laser induced nonsequential double ionization. Phys. Rev. Lett. **84**, 3546–3549 (2000)

Bergues, B., Kübel, M., Johnson, N.G., Fischer, B., Camus, N., Betsch, K.J., Herrwerth, O., Senftleben, A., Sayler, A.M., Rathje, T., Pfeifer, T., Ben-Itzhak, I., Jones, R.R., Paulus, G.G., Krausz, F., Moshammer, R., Ullrich, J., Kling, M.F.: Attosecond tracing of correlated electron-emission in non-sequential double ionization. Nat. Commun. **3**, 813 (2012)

Chen, Z.J., Liang, Y.Q., Lin, C.D.: Quantum theory of recollisional (e, 2e) process in strong field nonsequential double ionization of helium. Phys. Rev. Lett. **104**, 253201 (2010)

Corkum, P.B.: Plasma perspective on strong field multiphoton ionization. Phys. Rev. Lett. **71**, 1994–1997 (1993)

de Morisson Faria, C.F., Liu, X.: Electron-electron correlation in strong laser fields. J. Mod. Opt. **58**, 1076–1131 (2011)

Delone, N.B., Krainov, V.P.: Energy and angular electron spectra for the tunnel ionization of atoms by strong low-frequency radiation. J. Opt. Soc. Am. B **8**, 1207–1211 (1991)

DiChiara, A.D., Sistrunk, E., Blaga, C.I., Szafruga, U.B., Agostini, P., DiMauro, L.F.: Inelastic scattering of broadband electron wave packets driven by an intense midinfrared laser field. Phys. Rev. Lett. **108**, 033002 (2012)

Feuerstein, B., Moshammer, R., Fischer, D., Dorn, A., Schröter, C.D., Deipenwisch, J., Crespo Lopez-Urrutia, J.R., Höhr, C., Neumayer, P., Ullrich, J., Rottke, H., Trump, C., Wittmann, M., Korn, G., Sandner, W.: Separation of recollision mechanisms in nonsequential strong field double ionization of Ar: the role of excitation tunneling. Phys. Rev. Lett. **87**, 043003 (2001)

Fittinghoff, D.N., Bolton, P.R., Chang, B., Kulander, K.C.: Observation of nonsequential double ionization of helium with optical tunneling. Phys. Rev. Lett. **69**, 2642–2645 (1992)

Fu, L.B., Liu, J., Chen, J., Chen, S.G.: Classical collisional trajectories as the source of strong-field double ionization of helium in the knee regime. Phys. Rev. A **63**, 043416 (2001)

Haan, S.L., Breen, L., Karim, A., Eberly, J.H.: Variable time lag and backward ejection in full-dimensional analysis of strong-field double ionization. Phys. Rev. Lett. **97**, 103008 (2006)

Haan, S.L., Van Dyke, J.S., Smith, Z.S.: Recollision excitation, electron correlation, and the production of high-momentum electrons in double ionization. Phys. Rev. Lett. **101**, 113001 (2008a)

Haan, S.L., Smith, Z.S., Shomsky, K.N., Plantinga, P.W.: Anticorrelated electrons from weak recollisions in nonsequential double ionization. J. Phys. B **41**, 211002 (2008b)

Hao, X.L., Chen, J., Li, W.D., Wang, B.B., Wang, X.D., Becker, W.: Quantum effects in double ionization of argon below the threshold intensity. Phys. Rev. Lett. **112**, 073002 (2014)

He, M.R., Li, Y., Zhou, Y.M., Li, M., Lu, P.X.: Temporal and spatial manipulation of the recolliding wave packet in strong-field photoelectron holography. Phys. Rev. A **93**, 033406 (2016)

Herrwerth, O., Rudenko, A., Kremer, M., de Jesus, V.L.B., Fischer, B., Gademann, G., Simeonidis, K., Achtelik, A., Ergler, Th, Feuerstein, B., Schröter, C.D., Moshammer, R., Ullrich, J.: Wavelength dependence of sub-laser-cycle few-electron dynamics in strong-field multiple ionization. New J. Phys. **10**, 025007 (2008)

Hickstein, D.D., Ranitovic, P., Witte, S., Tong, X.M., Huismans, Y., Arpin, P., Zhou, X.B., Keister, K.E., Hogle, C.W., Zhang, B.S., Ding, C.Y., Johnsson, P., Toshima, N., Vrakking, M.J.J., Murnane, M.M., Kapteyn, H.C.: Direct Visualization of Laser-Driven Electron Multiple Scattering and Tunneling Distance in Strong-Field Ionization. Phys. Rev. Lett. **109**, 073004 (2012)

Ho, P.J., Panfili, R., Haan, S.L., Eberly, J.H.: Nonsequential double ionization as a completely classical photoelectric effect. Phys. Rev. Lett. **94**, 093002 (2005)

Hu, S.X.: Boosting photoabsorption by attosecond control of electron correlation. Phys. Rev. Lett. **111**, 123003 (2013)

Huang, C., Zh, M.M., Wu, Z.M.: Recollision dynamics in nonsequential double ionization of atoms by long-wavelength pulses. Opt. Express **24**, 28361–28371 (2016a)

Huang, C., Guo, W.L., Zhou, Y.M., Wu, Z.M.: Role of coulomb repulsion in correlated-electron emission from a doubly excited state in nonsequential double ionization of molecules. Phys. Rev. A **93**, 013416 (2016b)

Huang, H., Ke, S.L., Wang, B., Long, H., Wang, K., Lu, P.X.: Numerical study on plasmonic absorption enhancement by a rippled graphene sheet. J Lightwave Technol. **35**, 320–324 (2017)

I'Huillier, A., Lompre, L.A., Mainfray, G., Manus, C.: Multiply charged ions induced by multiphoton absorption in rare gases at 0.53 μm. Phys. Rev. A **27**, 2503–2512 (1983)

Ivanov, I.A., Kheifets, A.S., Calvert, J.E., Goodall, S., Wang, X., Xu, H., Palmer, A.J., Kielpinski, D., Litvinyuk, I.V., Sang, R.T.: Transverse electron momentum distribution in tunneling and over the barrier ionization by laser pulses with varying ellipticity. Sci. Rep. **6**, 19002 (2016)

Kübel, M., Kling, N.G., Betsch, K.J., Camus, N., Kaldun, A., Kleineberg, U., Ben-Itzhak, I., Jones, R.R., Paulus, G.G., Pfeifer, T., Ullrich, J., Moshammer, R., Kling, M.F., Bergues, B.: Nonsequential double ionization of N_2 in a near-single-cycle laser pulse. Phys. Rev. A **88**, 023418 (2013)

Lein, M., Gross, E.K.U., Engel, V.: Intense-field double ionization of helium: identifying the mechanism. Phys. Rev. Lett. **85**, 4707–4710 (2000)

Lewenstein, M., Balcou, Ph, Ivanov, MYu., L'Huillier, A., Corkum, P.B.: Theory of high-harmonic generation by low-frequency laser fields. Phys. Rev. A **49**, 2117–2132 (1994)

Li, Y.B., Wang, X., Yu, B.H., Tang, Q.B., Wang, G.H., Wan, J.G.: Nonsequential double ionization with mid-infrared laser fields. Sci. Rep. **6**, 37413 (2016)

Li, L., Wang, Z., Li, F., Long, H.: Efficient generation of highly elliptically polarized attosecond pulses. Opt. Quantum Electron. **49**, 73 (2017)

Liu, X., Rottke, H., Eremina, E., Sandner, W., Goulielmakis, E., Keeffe, K.O., Lezius, M., Krausz, F., Lindner, F., Schätzel, M.G., Paulus, G.G., Walther, H.: Nonsequential double ionization at the single-optical-cycle limit. Phys. Rev. Lett. **93**, 263001 (2004)

Liu, Y.Q., Tschuch, S., Rudenko, A., Dürr, M., Siegel, M., Morgner, U., Moshammer, R., Ullrich, J.: Strong-field double ionization of Ar below the recollision threshold. Phys. Rev. Lett. **101**, 053001 (2008)

Liu, J.L., Li, Y.F., Ding, L., Zhang, C.F., Fang, J.X.: A simple method for afterpulse probability measurement in high-speed single-photon detectors. Infrared Phys. Technol. **77**, 451–455 (2016)

Liu, X., Li, P.C, Zhu, X.S., Lan, P.F., Zhang, Q.B., Lu, P.X.: Probing the π-π* transitions in conjugated compounds with an infrared femtosecond laser. Phys. Rev. A **95**, 033421 (2017)

Ma, X.M., Zhou, Y.M., Lu, P.X.: Multiple recollisions in strong-field nonsequential double ionization. Phys. Rev. A **93**, 013425 (2016)

Mauger, F., Chandre, C., Uzer, T.: Strong field double ionization: the phase space perspective. Phys. Rev. Lett. **102**, 173002 (2009)

Maxwell, A.S., de Morisson, Figueira, Faria, C.: Controlling below-threshold nonsequential double ionization via quantum interference. Phys. Rev. Lett. **116**, 143001 (2016)

Moshammer, R., Feuerstein, B., Schmitt, W., Dorn, A., Schröter, C.D., Ullrich, J., Rottke, H., Trump, C., Wittmann, M., Korn, G., Hoffmann, K., Sandner, W.: Momentum distributions of Ne^{n+} ions created by an intense ultrashort laser pulse. Phys. Rev. Lett. **84**, 447–450 (2000)

Panfili, R., Eberly, J.H., Haan, S.L.: Comparing classical and quantum simulations of strong-field double-ionization. Opt. Expr. **8**, 431–435 (2001)

Parker, J.S., Doherty, B.J.S., Taylor, K.T., Schultz, K.D., Blaga, C.I., DiMauro, F.: High-energy cutoff in the spectrum of strong-field nonsequential double ionization. Phys. Rev. Lett. **96**, 133001 (2006)

Pullen, M.G., Wolter, B., Wang, X., Tong, X.M., Sclafani, M., Baudisch, M., Pires, H., Schröter, C.D. Ullrich,, J., Pfeifer, T., Moshammer, R., Eberly, J.H., Biegert, J.: Transition from non-sequential to sequential double ionisation in many-electron systems. arXiv:1602.07840 (2016)

Qin, M.Y., Zhu, X.S.: Molecular orbital imaging for partially aligned molecules. Opt. Laser Technol. **87**, 79–86 (2017)

Rudenko, A., Zrost, K., Feuerstein, B., de Jesus, V.L.B., Schröter, C.D., Moshammer, R., Ullrich, J.: Correlated multielectron dynamics in ultrafast laser pulse interactions with atoms. Phys. Rev. Lett. **93**, 253001 (2004)

Rudenko, A., de Jesus, V.L.B., Ergler, Th, Zrost, K., Feuerstein, B., Schröter, C.D., Moshammer, R., Ullrich, J.: Correlated two-electron momentum spectra for strong-field nonsequential double ionization of He at 800 nm. Phys. Rev. Lett. **99**, 263003 (2007)

Rudenko, A., Ergler, Th, Zrost, K., Feuerstein, B., de Jesus, V.L.B., Schröer, C.D., Moshammer, R., Ullrich, J.: Intensity-dependent transitions between different pathways of strong-field double ionization. Phys. Rev. A **78**, 015403 (2008)

Schöffler, M.S., Xie, X.H., Wustelt, P., Moller, M., Roither, S., Kartashov, D., Sayler, A.M., Baltuska, A., Paulus, G.G., Kitzler, M.: Laser-subcycle control of sequential double-ionization dynamics of helium. Phys. Rev. A **93**, 063421 (2016)

Staudte, A., Ruiz, C., Schöffler, M., Schössler, S., Zeidler, D., Weber, Th, Meckel, M., Villeneuve, D.M., Corkum, P.B., Becker, A., Dörner, R.: Binary and recoil collisions in strong field double ionization of helium. Phys. Rev. Lett. **99**, 263002 (2007)

Sun, X.F., Li, M., Ye, D.F., Xin, G.G., Fu, L.B., Xie, X.G., Deng, Y.K., Wu, C.Y., Liu, J., Liu, Y.Q.: Mechanisms of strong-field double ionization of Xe. Phys. Rev. Lett. **113**, 103001 (2014)

Tanaka, K., Miyamura, K., Akishima, K., Tonokura, K., Konno, M.: Sensitive measurements of trace gas of formaldehyde using a mid-infrared laser spectrometer with a compact multi-pass cell. Infrared Phys. Technol. **79**, 1–5 (2016)

Tang, Q.B., Zhou, Y.M., Huang, C., Liao, Q., Lu, P.X.: Correlated electron dynamics in nonsequential double ionization of molecules by mid-infrared fields. Opt. Express **20**, 19580–19588 (2012)

Tong, A.H., Zhou, Y.M., Lu, P.X.: Resolving subcycle electron emission in strong-field sequential double ionization. Opt. Express **23**, 15774–15783 (2015)

Tong, A.H., Zhou, Y.M., Lu, P.X.: Bifurcation of ion momentum distributions in sequential double ionization by elliptically polarized laser pulses. Opt. Quantum Electron. **49**, 77 (2017)

Walker, B., Sheehy, B., DiMauro, L.F., Agostini, P., Schafer, K.J., Kulander, K.C.: Precision measurement of strong field double ionization of helium. Phys. Rev. Lett. **73**, 1227–1230 (1994)

Wang, Z., Li, M., Zhou, Y.M., Lan, P.F., Lu, P.X.: Correlated electron-nuclear dynamics in above-threshold multiphoton ionization of asymmetric molecule. Sci. Rep. **7**, 42585 (2017a)

Wang, F., Qin, C.Z., Wang, B., Long, H., Wang, K., Lu, P.X.: Rabi Oscillations of Plasmonic Supermodes in Graphene Multilayer Arrays. IEEE J Sel Top Quant **23**, 1 (2017b)

Wang, X., Eberly, J.H.: Effects of elliptical polarization on strong-field short-pulse double ionization. Phys. Rev. Lett. **103**, 103007 (2009)

Weber, Th, Giessen, H., Weckenbrock, M., Urbasch, G., Staudte, A., Spielberger, L., Jagutzki, O., Mergel, V., Vollmer, M., Dörner, R.: Correlated electron emission in multiphoton double ionization. Nat. (Lond.) **405**, 658–661 (2000)

Weckenbrock, M., Becker, A., Staudte, A., Kammer, S., Smolarski, M., Bhardwaj, V.R., Rayner, D.M., Villeneuve, D.M., Corkum, P.B., Dörner, R.: Electron-electron momentum exchange in strong field double ionization. Phys. Rev. Lett. **91**, 123004 (2003)

Wolter, B., Pullen, M.G., Baudisch, M., Sclafani, M., Hemmer, M., Senftleben, A., Schröter, C.D., Ullrich, J., Moshammer, R., Biegert, J.: Strong-field physics with mid-IR fields. Phys. Rev. X **5**, 021034 (2015)

Xu, T.T., Ben, S., Wang, T., Zhang, J., Guo, J., Liu, X.S.: Exploration of the nonsequential double-ionization process of a Mg atom with different delay time in few-cycle circularly polarized laser fields. Phys. Rev. A **92**, 033405 (2015)

Ye, D.F., Liu, X., Liu, J.: Classical trajectory diagnosis of a fingerlike pattern in the correlated electron momentum distribution in strong field double ionization of helium. Phys. Rev. Lett. **101**, 233003 (2008)

Yuan, Z.Q., Ye, D.F., Liu, J., Fu, B.: Inner-shell electron effects in strong-field double ionization of Xe. Phys. Rev. A **93**, 063409 (2016)

Zhai, C.Y., He, L.X., Lan, P.F., Zhu, X.S., Li, Y., Wang, F., Shi, W.J., Zhang, Q.B., Lu, X.: Coulomb-corrected molecular orbital tomography of nitrogen. Sci. Rep. **6**, 23236 (2016)

Zhai, C.Y., Zhu, X.S., Lan, P.F., Wang, F., He, L.X, Shi, W.J., Li, Y., Li, M., Zhang, Q.B., Lu, P.X.: Diffractive molecular-orbital tomography. Phys. Rev. A **95**, 033420 (2017)

Zhang, L., Xie, X.H., Roither, S., Zhou, Y.M., Lu, P.X., Kartashov, D., Schöffler, M., Shafir, D., Corkum, P.B., Baltuška, A., Staudte, A., Kitzler, M.: Subcycle control of electron-electron correlation in double ionization. Phys. Rev. Lett. **112**, 193002 (2014)

Zhang, X.F., Zhu, X.S., Liu, X., Wang, D., Zhang, Q.B., Lan, P.F., Lu, P.X.: Ellipticity-tunable attosecond XUV pulse generation with a rotating bichromatic circularly polarized laser field. Opt. Lett. **42**, 1027–1030 (2017)

Zhou, Y.M., Liao, Q., Lu, P.X.: Mechanism for high-energy electrons in nonsequential double ionization below the recollision-excitation threshold. Phys. Rev. A **80**, 023412 (2009)

Zhou, Y.M., Liao, Q., Lu, P.X.: Asymmetric electron energy sharing in strong-field double ionization of helium. Phys. Rev. A **82**, 053402 (2010)

Zhou, Y.M., Huang, C., Lu, X.: Coulomb-tail effect of electron-electron interaction on nonsequential double ionization. Phys. Rev. A **84**, 023405 (2011a)

Zhou, Y.M., Huang, C., Tong, A.H., Liao, Q., Lu, P.X.: Correlated electron dynamics in nonsequential double ionization by orthogonal two-color laser pulses. Opt. Express **19**, 2301–2308 (2011b)

Zhou, Y.M., Huang, C., Liao, Q., Lu, P.X.: Classical simulations including electron correlations for sequential double ionization. Phys. Rev. Lett. **109**, 053004 (2012)

Zhou, Y.M., Tolstikhin, O.I., Morishita, T.: Near-forward rescattering photoelectron holography in strong-field ionization: extraction of the phase of the scattering amplitude. Phys. Rev. Lett. **116**, 173001 (2016)

Zhu, X.S., Lan, P.F., Liu, K.L., Li, Y., Liu, X., Zhang, Q.B., Barth, I., Lu, P.X.: Helicity sensitive enhancement of strong-field ionization in circularly polarized laser fields. Opt. Express **24**, 4196–4209 (2016)